OPEN

NPG Asia Materials (2017) 9, e424; doi:10.1038/am.2017.148
www.nature.com/am

ORIGINAL ARTICLE

Quantum-well-induced engineering of magnetocrystalline anisotropy in ferromagnetic films

Ching-Hao Chang[1,2,5], Kun-Peng Dou[1,5,6], Guang-Yu Guo[3] and Chao-Cheng Kaun[1,4]

Tuning quantum well states (QWSs) to govern physical properties in nanoscale leads to the development of advanced electronic devices. Here, we propose that QWSs can be engineered to control magnetocrystalline anisotropy energy (MCAE) which dominates the magnetization orientation (that is, the easy axis) of a ferromagnetic thin film. We investigate from first-principles the MCAE of the bcc Fe film on an Ag substrate. The calculated MCAE oscillates largely as Fe thickness increases agreeing well with experiments, and reaches oscillation extremes as the Fe d-orbital QWSs approach the Fermi level (E_F). Crucially, we find that this phenomenon stems from the combined effect of intrinsic spin-orbit interaction (SOI) and Rashba SOI field on the Fe QWSs, which modulates the density of states at E_F as the Fe thickness varies. Moreover, this effect offers a way to tune not only the strength of magnetic anisotropy but also the easy axis of a Fe film by shifting E_F within ten meV via moderately charge injection, which could realize advanced memory devices with ultra-low power consumption.
NPG Asia Materials (2017) **9,** e424; doi:10.1038/am.2017.148; published online 25 August 2017

INTRODUCTION

Discovery of novel magnetic properties triggers the development of spintronics. For examples, the giant and tunneling magnetoresistance effects are applied in the data storage technology, exponentially boosting the capability of memory devices,[1–4] and the spin transfer torque is used to achieve nonvolatile magnetoresistive random access memory devices.[5–7] All these properties hinge directly on one quantity: the magnetic anisotropy energy (MAE).[8,9] It stems from both the magnetic dipole and the magnetocrystalline anisotropy energy (MCAE), while the latter dominates the nature of anisotropy in nanoscale systems.[10]

The ability to engineer the MCAE by altering the film thickness is important in reducing the size of memory devices to increase the storage density,[11,12] and to tune the MCAE to switch easy axis by injecting a small amount of charge is key in developing memory devices with ultra-low power consumption.[13] Since the Fe film is a building block for memory and spintronics devices, tailoring the MCAE of a Fe film by above routes gathers great interests. The magnitude of MCAE is observed to oscillate strongly with the increase of Fe film thickness.[14,15] This oscillatory feature relates to the impact of quantum well states (QWSs), as the oscillatory magnetic coupling in GMR systems,[16–18] but which and why QWSs cause it is still under debate.[19–21] Besides, the value of MAE is measured to increase remarkably by applying a small electric field to charge a Fe film moderately.[13] Such property has great application potential as it persists to a Fe film thicker than 1 nm,[22,23] even though the field is strongly screened in such a thick film. A recent experiment reveals a link between this property and QWSs,[22] but the detailed mechanism remains a puzzle.

In this work, we demonstrate that the above features are generated by the same species of Fe QWSs. We investigate the MCAE in Fe thin films on an Ag substrate from first principles. The calculated MCAE oscillates strongly as a function of Fe thickness, where extremes of the MCAE oscillation are consistent with experimental data.[14,15] By analyzing the spectra of Fe d-orbital QWSs in such a system, we find that only the minority QWSs appear near E_F when the Fe thickness is smaller than 10 monolayers (MLs). As the minority QWSs locate at E_F, they generate the oscillation extremes due to the effect of spin orbital interaction (SOI). For the thickness of Fe becomes larger than 10 MLs; however, both minority and majority QWSs approach E_F. The band intersections of both QWSs generate the oscillation extremes due to the combined effect of SOI and interfacial Rashba field. Although interfacial Rashba field is known to affect the interface or surface states,[24] here we demonstrate that it also influences the bulk QWSs and thus impacts the bulk physical properties, agreeing with recent observations.[25–27]

Since the MCAE oscillation correlates with the Fe-QWS position respecting to E_F, the MCAE can be tailored by moderately charging the Fe film to shift E_F. We propose that magnitude of MCAE can be modified by several times by charging a Fe film within one electron per unit cell and the magnetization orientation of a 5-MLs Fe film can be switched.

[1]Research Center for Applied Sciences, Academia Sinica, Taipei, Taiwan; [2]Institute for Theoretical Solid State Physics, Leibniz-Institute for Solid State and Materials Research, Dresden, Germany; [3]Department of Physics, National Taiwan University, Taipei, Taiwan and [4]Department of Physics, National Tsing Hua University, Hsinchu, Taiwan
[5]These authors contributed equally to this work.
[6]Current address: College of Information Science and Engineering, Ocean University of China, Qingdao 266100, China.
Correspondence: Dr C-H Chang or C-C Kaun, Research Center for Applied Sciences, Academia Sinica, 128 Sec. 2, Academia Road, Nankang, Taipei 11529, Taiwan.
E-mail: cutygo@gmail.com or kauncc@gate.sinica.edu.tw
Received 1 February 2017; revised 26 May 2017; accepted 21 June 2017

MATERIALS AND METHODS

Our first-principles calculations were carried out within the density functional theory (DFT) with the generalized gradient approximation (GGA). The accurate projector-augmented wave (PAW) method, as implemented in the Vienna ab initio simulation package (VASP), was used. The 5-MLs Ag slab was used as the substrate, which should be sufficient for the MCAE calculations for the Fe film on Ag.[19] Adopting the measured structural parameters of the Fe/Au system, the distance between the neighboring Fe–Fe layers was set to 1.41 Å and that between the Fe–Ag layers was set to 1.76 Å, respectively,[28] as the Ag and Au share the same fcc lattice and have almost identical lattice constants. The distance between the Fe edge layers of 1.39 Å was used. In the present self-consistent electronic structure and total energy calculations, the Brillouin zone summation was performed with a $20\times20\times1k$-point grid, the plane-wave energy cutoff of 300 eV was used, and the convergence criteria was less than 10^{-6} eV.

RESULTS

Magnetocrystalline and magnetic anisotropy energies

The MCAE in ferromagnetic thin films is understood from the perturbation theory where the SOI couples two electronic states with either the same or opposite spins.[10,20,29–31] The states with the same spin have higher possibility to interact with each other by overlapping their bands, since ferromagnetism lifts the spin degeneracy. Thus the effect of the SOI between the same spin states with different orbitals (intra-spin SOI) is the focus of research.[21,32,33] However, the SOI between different spin states (inter-spin SOI) can be crucial when a specific ferromagnetic thin film is considered, since the interface charge transfer between film and substrate induces the Rashba SOI field.[34] This field can enhance the impact of inter-spin SOI on the MCAE by increasing the possibility of spin-flip scattering.[35]

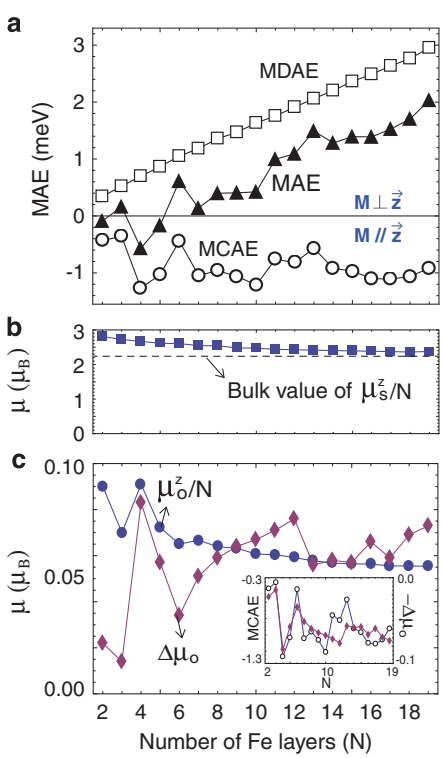

Figure 1 Magnetic anisotropy and magnetic moments of Fe_N films on Ag substrate. (**a**) Calculated MCAE (rings), MDAE (squares) and MAE (triangles) as a function of the Fe thickness (N). (**b**) Calculated average spin magnetic moment per Fe atom in the $M||\vec{z}$ state. The dashed line denotes the bulk value of 2.25 μ_B measured recently.[40] (**c**) Calculated average orbital magnetic moment per Fe atom in the $M||\vec{z}$ state (circles) and orbital magnetic moment anisotropy (diamonds). The inset shows that the correlation between the orbital magnetic moment anisotropy and MCAE. The solid lines are a guide to the eye only.

We consider a junction containing a N MLs Fe film with an Ag substrate to include the effect of Rashba field, and the surface normal is along the (001) direction (the z axis). The Fe_N/Ag junction is in either the $M||\vec{z}$ or $M\perp\vec{z}$ magnetic states when the Fe magnetization is along the z direction or in the x-y plane (the $M\parallel\vec{x}$ is fixed in the plane), respectively. The MCAE is then defined as the energy difference between $M||\vec{z}$ and $M\perp\vec{z}$ states, (E_z–E_x), and is calculated as a function of the Fe thickness (Figure 1a). Using the calculated magnetic moments, the magnetic dipole anisotropy energy (MDAE) is also evaluated by Ewald's lattice summation technique,[36] as shown in Figure 1a. In contrast to the MCAE which is generally negative (that is, prefering $M||\vec{z}$) and oscillates with thickness N,[19,37] the MDAE is always positive (that is, prefering $M\perp\vec{z}$) and increases with thickness N. Their sum leads to the nearly negative total MAE (that is, perpendicular magnetic anisotropy) when $N\leqslant 5$. Interestingly, the MAE becomes positive and the junction switches to the $M\perp\vec{z}$ state as $N\geqslant 6$. This result agrees rather well with the measured MAE of a Fe film on Ag (001).[14,38–40] In addition, the result indicates another spin-reorientation transition occurring between $N=2$ and 4 (Figure 1a) that is also reported recently.[41]

The junctions with Fe thickness $N=4$, 10 and 16 give rise to the MCAE minimums, as shown in Figure 1a, leading to a period of 6 MLs in the MCAE oscillation, agreeing well with available experimental results.[15,42] Furthermore, the minimum at $N=10$, the maximum at $N=13$, and the oscillation profile from $N=9$ to 18 are all in good agreement with the measured MAE. This is the first time that the first-principles density functional calculations reproduce well the MAE oscillation measured in the Fe/Ag (001) junction.[20] Nevertheless, the measured MAE is reported to decrease with N,[14,15] which is inconsistent with the calculated MAE shown in Figure 1a. This discrepancy could be due to the fact that in the experiments,[14,15] the Fe films were deposited on the stepped surface rather than on the atomically flat surface as assumed in this work.[43] Such a step geometry was found to stabilize the $M||\vec{z}$ state[39] and thus could substantially enhance the amplitude of MAE oscillation.[43]

To understand the origin of MCAE oscillation, we calculate the averaged spin magnetic moment (μ_S/N). We find that the calculated μ_S/N increases monotonically as the Fe layer becomes thinner, because μ_S of the Fe atoms on the surface and interface layers are considerably enhanced (Figure 1b and Supplementary Table S1).[40,44] Therefore, the behavior of spin magnetic moment cannot be correlated with the MCAE oscillation. We further evaluate the orbital magnetic moment anisotropy $\Delta\mu_o=(\mu_o^z-\mu_o^x)$ as a function of N. Clearly, the calculated $\Delta\mu_o$ is oscillatory and is closely related to the MCAE oscillation (see the inset in Figure 1c). Such a correlation was also observed in a recent experiment.[15] This indicates that the SOI leads to the MCAE oscillation through perturbing the $M||\vec{z}$ and $M\perp\vec{z}$ states differently.[30,45] The calculated μ_S and μ_0 on all Fe atoms in the $M||\vec{z}$ state are provided in Supplementary Tables S1 and S2, respectively. Furthermore, comparisons between our theoretical results and available measurements on the MAE and on the orbital magnetic moment anisotropy are made in Supplementary Figures S1 and S2. Besides, we also calculate MCAE in the optimized lattice structure and the results are consistent with those in the measured lattice structure (Supplementary Figure S3).

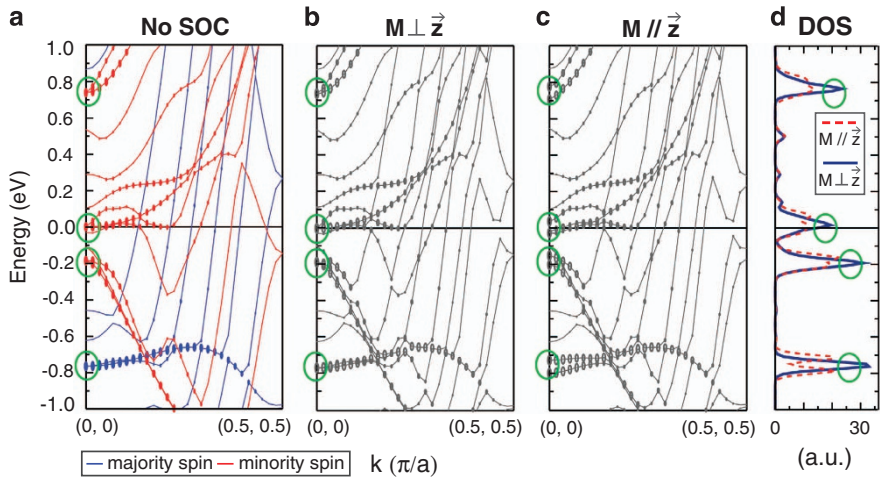

Figure 2 Band structures and density of states (DOS) of the Fe_4/Ag bilayer. Band structures of the system (**a**) without SOI, (**b**) with SOI ($M\perp\vec{z}$), and (**c**) with SOI ($M||\vec{z}$). Weights of d_{xz} and d_{yz} orbitals are projected to the majority (blue) and minority (red) spin bands. (**d**) DOS of the system close to the Γ point.

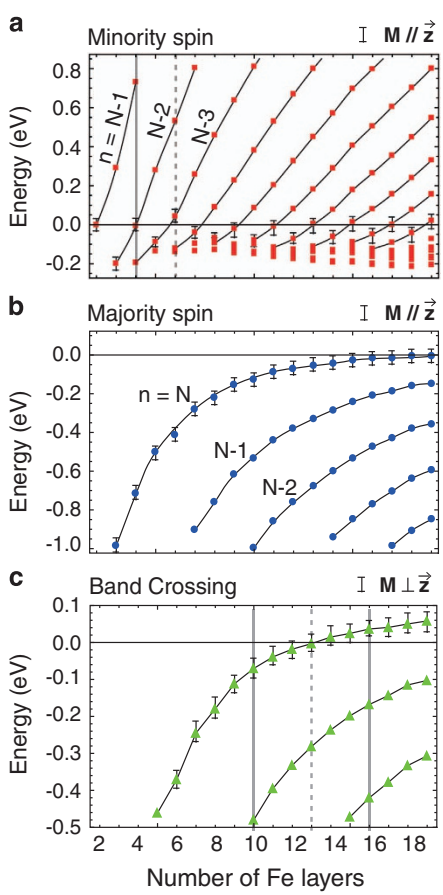

Figure 3 Energies of Fe QWSs and their band crossings versus Fe thickness. (**a**, **b**) Energies of minority (majority) spin QWSs at the Γ point in the $M\perp\vec{z}$ state labeled by squares (circles), and those in $M||\vec{z}$ denoted by short horizontal lines. The QWSs with quantum number $n=N-l$, where l is an integer, are joined by black lines. (**c**) Energies of band crossings between the minority and majority spin Fe QWSs. In contrast to (**a**, **b**), the energies of band crossings in the $M||\vec{z}$ state are labeled by triangles, and those split in the $M\perp\vec{z}$ state are denoted by short horizontal lines. The locations of MCAE maximums (minimums) are denoted by the gray solid (dashed) lines.

Effects of the intrinsic spin-orbit interaction

For the Fe thin film confined in the Z direction, the majority and minority spin bands of Fe d_{xz}, d_{yz} and $d_{3z^2-r^2}$ orbitals would form standing waves, that is, QWSs. The QWSs with Fe d_{xz} and d_{yz} orbitals, having a higher magnetic quantum number ($m=\pm 1$), are more susceptible to the intrinsic SOI compared with those of the $d3z^2-r^2$ orbital ($m=0$), and thus play a key role in the MCAE oscillation.[15]

To understand the minimum of the MCAE oscillation at the Fe_4 film shown in Figure 1a, we plot its band structures in different magnetic states with the contributions of the Fe d_{xz} and d_{yz} states highlighted in Figure 2. When the SOI is absent, the system has no preferred magnetization orientation, and the d_{xz}- and d_{yz}-orbital QWSs are doubly degenerate at the Γ point (see circles in Figure 2a) due to the film geometry. Turning on the SOI, the degeneracy is broken and the d_{xz}- and d_{yz}-orbital bands are split. The magnitudes of the splitting for the $M||\vec{z}$ and $M\perp\vec{z}$ states are very different (Figure 2b and c).

The SOI perturbs the system through the Hamiltonian $\mathcal{H}_{SO}=\lambda_{so}L\times S=\lambda_{so}[L_+\sigma_-+L_-\sigma_++L_z\sigma_z]/2$, where λ is the SOI constant depending on the material[29] and σ is the Pauli matrix. For orbitals $d_{xz}=\{|-1\rangle-|1\rangle\}/\sqrt{2}$ and $d_{yz}=i\{|-1\rangle+|1\rangle\}/\sqrt{2}$, the matrix elements of operator $L_\pm$ are all zero in the $\{d_{xz}, d_{yz}\}$ basis, hence the d_{xz} and d_{yz} QWSs are only affected by the z component of $\mathcal{H}_{SO}$

$$\mathcal{H}_{SO}^{eff}=\mathcal{H}_{SO}^{(z)}=\lambda_{so}L_z\sigma_z/2. \quad (1)$$

In the $M||\vec{z}$ state, the d_{xz} and d_{yz} QWSs near E_F are of the minority spin (that is, the spin $|\downarrow\rangle$ state), and the operator $\mathcal{H}_{SO}^{(z)}$ affects the d_{xz} and d_{yz} QWSs by first order perturbation of operator $\lambda_{so}L_z/2$ which leads to a large energy gap of ~60 meV considering the value of λ_{SO} of iron (see circles at Γ point in Figure 2c). For the $M\perp\vec{z}$ state (the magnetization along the x axis), the Fe d_{xz} and d_{yz} QWSs near E_F are of the minority spin and the spin state is $|\uparrow-\downarrow\rangle/\sqrt{2}$. Consequently, the first order perturbation of $\mathcal{H}_{SO}^{(z)}$ on the d_{xz} and d_{yz} QWSs becomes zero since $\langle\uparrow-\downarrow|\sigma_z|\uparrow-\downarrow\rangle=0$. Therefore, the induced energy gap reduces to merely few meV (see circles in Figure 2b).

Since the energy gaps at the Γ are located at the bottoms of the QWS bands which provide a large amount of density of states (DOS), their occurrence due to the change of magnetization direction affects

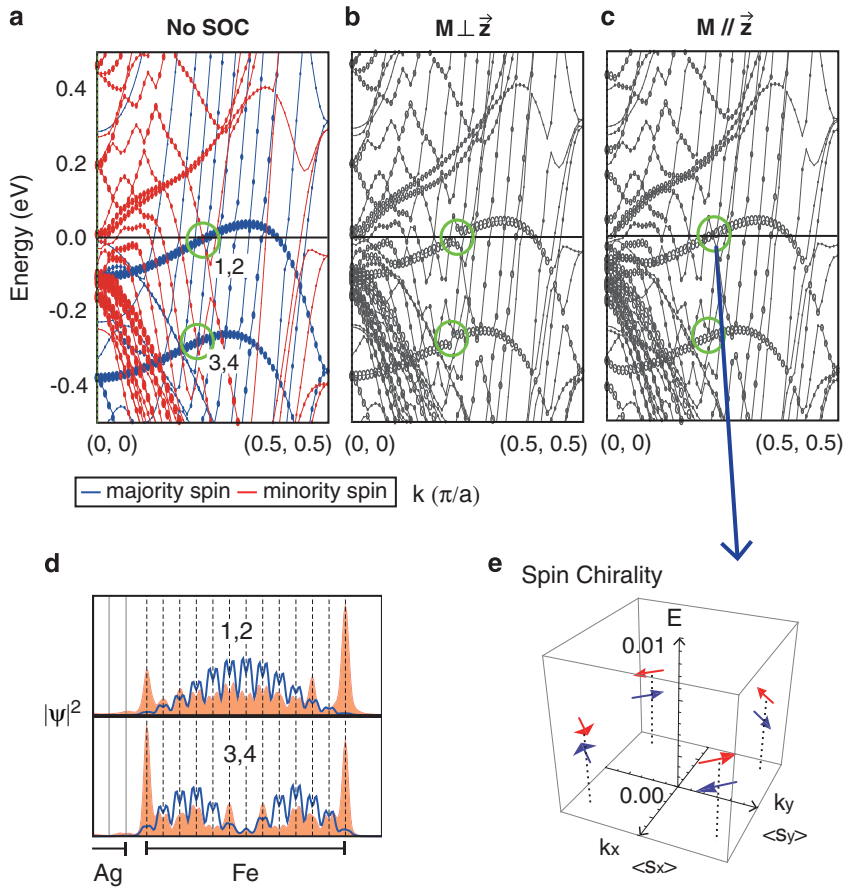

Figure 4 Band structures, charge densities, and spin chirality of the Fe_{13}/Ag bilayer. Band structures of the system (**a**) without SOI, (**b**) with SOI ($M\perp\vec{z}$) and (**c**) with SOI ($M||\vec{z}$). (**d**) Plane-averaged charge densities of doubly degenerate minority and majority spin QWSs circled in (**a**). (**e**) Spin projections of the QWSs that are split by SOI in (**c**). Spins of QWSs in all four quadrants of momentum frame are shown. The blue (red) refers to the positive (negative) out-plane spin $\langle s_z \rangle$, and the direction denotes the in-plane spin $\{\langle s_x \rangle, \langle s_y \rangle\}$.

the MCAE significantly. When the band bottom appears at E_F in the Fe_4/Ag junction, as displayed in Figure 2a, the SOI splits the DOS peak into one above and one below the E_F, resulting in a much reduced DOS at E_F in the $M||\vec{z}$ state (Figure 2d). In contrast, the DOS peak in the $M\perp\vec{z}$ state remains at E_F due to the much weaker higher order perturbation of the SOI. As a result, the energy E_z decreases, so that the MCAE (E_z–E_x) decreases, leading to the minimum at $N=4$ in the MCAE oscillation shown in Figure 1a.

To further understand the MCAE oscillation, Figure 3a shows the calculated energies of the minority QWSs at the Γ as a function of Fe thickness. There is one (two) averaged energy value (values) of QWSs in the $M\perp\vec{z}$ ($M||\vec{z}$) state, denoted by squares (horizontal lines), as the corresponding DOS peak is hardly (pronouncedly) split by the SOI. The MCAE decreases (increases) significantly as the DOS peak induced by the QWSs in the $M\perp\vec{z}$ ($M||\vec{z}$) state approaches E_F. Therefore, when $N=4$ (6), the square (the horizontal line) aligns with E_F, giving rise to the minimum (maximum) of MCAE.

Effects of the Rashba spin-orbit interaction field

When the Fe thickness is larger than 10 MLs, the majority spin QWSs also approach E_F (circles and horizontal lines, Figure 3b), and thus both the majority and minority spin QWSs can affect the MCAE. To understand the MCAE oscillation in this region, Figure 4a plots the band structures of the Fe_{13} in different magnetic states. The majority spin QWS band crosses E_F and contributes a large amount of DOS,[15] so that it dominates the total energy and MCAE over the minority spin QWS bands around the Γ point. Such majority spin band at E_F interacts with the minority spin band quite differently in the $M||\vec{z}$ and $M\perp\vec{z}$ states. For the $M\perp\vec{z}$ state, the spins of majority and minority are the basis of Paul matrix σ_x, namely, $|\uparrow \pm \downarrow\rangle/\sqrt{2}$. The spin states couple with each other by the σ_z in the effective SOI operator Equation (1) in the first order approximation, resulting in the gap opening of ~50 meV at E_F in Figure 4b. In contrast, no spin gap occurs in the $M||\vec{z}$ state, since the spin states in such state are the basis of σ_z, namely, $|\uparrow\rangle$ and $|\downarrow\rangle$. There is no spin-flip interaction in the first order perturbation of the operator $\mathcal{H}_{SO}^{(z)}$, and the spin gap in the $M||\vec{z}$ state is an order of magnitude smaller since it is the second order perturbation.

The large gap in the majority spin band in the $M\perp\vec{z}$ state reduces the DOS at E_F (Figure 4b) and thus lowers the total energy E_x, resulting in a peak in the MCAE (E_z–E_x) as shown in Figure 1a. As the Fe film is increased (reduced) to Fe_{16} (Fe_{10}), the crossing between different spin bands moves to 0.04 eV above (0.06 eV below) the E_F in the $M||\vec{z}$ state (Figure 3c). The large gap formation in the $M\perp\vec{z}$ state increases the total energy of E_x by moving the majority spin band downward to E_F to increase the DOS, generating the minimum of the MCAE oscillation at Fe_{16} shown in Figure 1a. We note that only certain minority spin bands can strongly interact with the majority spin bands, leading to the large energy gaps (see the green circles in Figure 4b). This is due to the requirement of strong inter-band

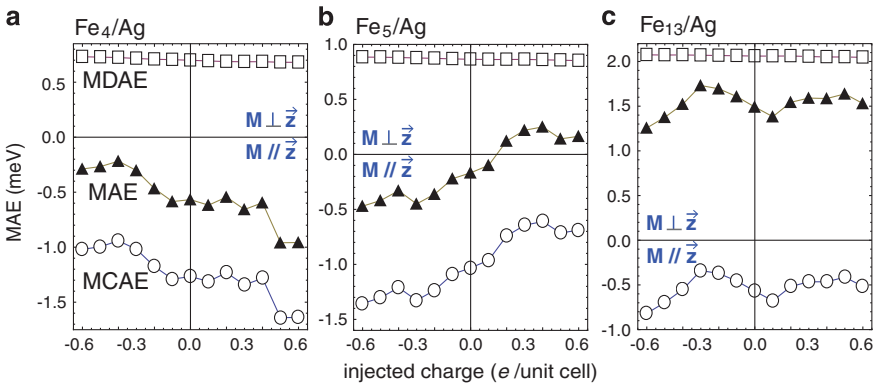

Figure 5 Magnetic anisotropy of (**a**) Fe_4/Ag, (**b**) Fe_5/Ag and (**c**) Fe_{13}/Ag junctions with different injected charges. The MCAE (rings), MDAE (squares) and MAE (triangles) are plotted versus Fe thickness (N).

interaction that the wavefunctions of both bands must have the same spatial parity and also overlap strongly (Figure 4d).

Although the energy gaps in Figure 4b are caused by the intrinsic SOI, it is crucially impacted by the Rashba SOI field, which comes from the Fe–Ag interface (see red line in Supplementary Figure S6) and dramatically increases the possibility of the spin-flip scattering. The field increases the gap in the $M \perp \vec{z}$ state by almost 70% compared with that in the free-standing Fe thin film (Supplementary Figures S4 and S5), and generates the in-plane chiral spin texture at the gap in the $M || \vec{z}$ state (Figure 4**c** and e). Such spin texture driven by the Rashba field is widely observed in non-magnetic systems,[46,47] and is eliminated in the present Fe film on Ag in the $M \perp \vec{z}$ state because the magnetization breaks the time reversal symmetry at the *x*-*y* plane. Here, we note that energy gaps in both Figure 2c and Figure 4b are around 50 meV, corresponding to a temperature of 600 K and ensuring the MAE oscillation measurements at a temperature of 200 K.[14,22] The Rashba parameter α_R can be estimated as 0.03 eV Å (Supplementary Section S3), which is close to the measured one in Pb thin films.[48]

Engineering the magnetocrystalline anisotropy energy by surface charging

The MCAE can be tuned efficiently by injecting charges into the Fe thin film by utilizing the direct relation between the MCAE and the Fe QWSs. In contrast, the MDAE is hardly affected by such charge injection. Indeed, Figure 5 shows that the values of MDAE of different Fe_N/Ag junctions slowly decrease with the increases of charges (around 7% in the whole range of plot), since the Fe d-orbital is more than half-filled. As a result, the MAE (the sum of MCAE and MDAE) in the Fe_4/Ag junction can be increased (reduced) by as much as 70 (60)% when the junction is charged by 0.5 (−0.4) e per unit cell, because of the increased (reduced) DOS difference between two magnetic states when raising (lowering) the E_F by about 15 (10) meV. The MAE changes more than four times in the whole range shown in Figure 5a, and its minimum (maximum) directly relates to the DOS peak near the E_F in the $M \perp \vec{z}$ ($M || \vec{z}$) state (Supplementary Figure S7).

Moreover, not only the magnitude but also the sign of MAE can be controlled in Fe_5/Ag junction by injecting charges. For such a Fe film with a Fe-minority QWS 10 meV below E_F, decreasing charges moves this QWS toward E_F to boost the magnitudes of MCAE and MAE, and increasing charges shifts the QWS away from E_F to decrease the MCAE, which finally switches the sign of MAE, leading to the change of easy axis (Figure 5b). Surprisingly, the remarkable change of MAE by injected charges can be also realized in a Fe film thicker than 1 nm such as Fe_{13}/Ag junction, where the band crossing of minority and majority QWSs locates at E_F. Although the injected charges only leads to a few meV shifting of E_F in Fe_{13}/Ag junction due to strongly screening effect therein, the MCAE and MAE can vary two times and 40%, respectively (Figure 5c). So far it has been measured that the MAE magnitude changes remarkably (around 40%) by tuning applied voltage to inject charges on a Fe film.[13,22,23] Our results explain the microscopic origin, show that the MAE of a Fe film can be boosted by several times and hence the magnetization orientation can be switched by injecting charges to shift the QWSs near E_F.

DISCUSSION

The calculated MAE in the Fe/Ag junction oscillates with the Fe thickness. The predicted period and extremes of this oscillation agree well with the available experiments. Importantly, by analyzing the band structures and DOS of the junction in the perpendicular and in-plane magnetizations, we find that the QWSs of Fe d_{xz} and d_{yz} orbitals induce the MCAE oscillation, as these QWSs are susceptible to the intrinsic SOI and also Rashba SOI field. Furthermore, our results also reveal that the QWSs of Fe d orbitals are also responsible for the fact that the MCAE can be largely tuned by a moderate charge injection, observed recently on the Fe films that the MCAE is sensitive to the applied gate voltage.[13] This work therefore provides a novel route to design ferromagnetic thin films with a desired MAE and magnetization orientation by fine tuning of the thickness, interface and injected charge, for advanced spintronics devices.

CONFLICT OF INTEREST

The authors declare no conflict of interest.

ACKNOWLEDGEMENTS

We thank TR Chang, W Ji, CM Wei and HT Jeng for valuable comments and discussions. This work was partially supported by the Ministry of Science and Technology, Taiwan through grants no 104-2112-M-001-008-MY3 and no 104-2112-M-002-002-MY3, and also the Future and Emerging Technologies (FET) program within the Seventh Framework Programme for Research of the European Commission, under FET-Open grant no 618083 (the CNTQC project).

Author contributions: C-HC and C-CK conceived and designed the project. The calculations were performed by K-PD, C-HC and G-YG. The manuscript was written by C-HC, G-YG and C-CK. All the authors contributed to the analysis and interpretation of the results.

PUBLISHER'S NOTE

Springer Nature remains neutral with regard to jurisdictional claims in published maps and institutional affiliations.

1 Baibich, M. N., Broto, J. M., Fert, A., Petroff, F., Etienne, P., Nguyen Van Dau, F., Creuzet, G., Friederich, A. & Chazelas, J. Giant magnetoresistance of (001)Fe/(001)Cr magnetic superlattices. *Phys. Rev. Lett.* **61**, 2472–2475 (1988).
2 Binasch, G., Grünberg, P., Saurenbach, F. & Zinn, W. Enhanced magnetoresistance in layered magnetic structures with antiferromagnetic interlayer exchange. *Phys. Rev. B* **39**, 4828–4830 (1989).
3 Miyazaki, T. & Tezuka, N. Giant magnetic tunneling effect in Fe/Al_2O_3/Fe junction. *J. Magnet. Magnet. Mater.* **139**, L231–L234 (1995).
4 Moodera, J. S., Kinder, L. R., Wong, T. M. & Meservey, R. Large magnetoresistance at room temperature in ferromagnetic thin film tunnel junctions. *Phys. Rev. Lett.* **74**, 3273–3276 (1995).
5 Slonczewski, J. C. Conductance and exchange coupling of two ferromagnets separated by a tunneling barrier. *Phys. Rev. B* **39**, 6995–7002 (1989).
6 Fang, D., Kurebayashi, H., Wunderlich, J., Výborný, K., Zârbo, L. P., Campion, R. P., Casiraghi, A., Gallagher, B. L., Jungwirth, T. & Ferguson, A. J. Spin-orbit-driven ferromagnetic resonance. *Nat. Nanotech.* **6**, 413–417 (2011).
7 Sankey, J. C., Cui, Y. T., Sun, J. Z., Slonczewski, J. C., Buhrman, R. A. & Ralph, D. C. Measurement of the spin-transfer-torque vector in magnetic tunnel junctions. *Nat. Phys.* **4**, 67–71 (2008).
8 Carcia, P. F., Meinhaldt, A. D. & Suna, A. Perpendicular magnetic anisotropy in Pd/Co thin film layered structures. *Appl. Phys. Lett.* **47**, 178 (1985).
9 Wang, W.-G., Li, M., Hageman, S. & Chien, C. L. Electric-field-assisted switching in magnetic tunnel junctions. *Nat. Mater.* **11**, 64–68 (2012).
10 Smogunov, A., Dal Corso, A., Delin, A., Weht, R. & Tosatti, E. Colossal magnetic anisotropy of monatomic free and deposited platinum nanowires. *Nat. Nanotech.* **3**, 22–25 (2008).
11 Sun, J. Z., Trouilloud, P. L., Gajek, M. J., Nowak, J. & Robertazzi, R. P. Size dependence of spin-torque induced magnetic switching in CoFeB-based perpendicular magnetization tunnel junctions (invited). *J. Appl. Phys.* **111**, 07C711 (2012).
12 Kent, A. D. & Worledge, D. C. A new spin on magnetic memories. *Nat. Nanotech.* **10**, 187–191 (2015).
13 Maruyama, T., Shiota, Y., Nozaki, T., Ohta, K., Toda, N., Mizuguchi, M., Tulapurkar, A.A., Shinjo, T., Shiraishi, M., Mizukami, S., Ando, Y & Suzuki, Y Large voltage-induced magnetic anisotropy change in a few atomic layers of iron. *Nat. Nanotech.* **4**, 158–161 (2009).
14 Li, J., Przybylski, M., Yildiz, F., Ma, X. D. & Wu, Y. Z. Oscillatory magnetic anisotropy originating from quantum well states in Fe films. *Phys. Rev. Lett.* **102**, 207206 (2009).
15 Dabrowski, M., Peixoto, T. R. F., Pazgan, M., Winkelmann, A., Cinal, M., Nakagawa, T., Takagi, Y., Yokoyama, T., Bisio, F., Bauer, U., Yildiz, F., Przybylski, M. & Kirschner, J. Oscillations of the orbital magnetic moment due to *d*-band quantum well states. *Phys. Rev. Lett.* **113**, 067203 (2014).
16 Parkin, S. S. P., Bhadra, R. & Roche, K. P. Oscillatory magnetic exchange coupling through thin copper layers. *Phys. Rev. Lett.* **66**, 2152–2155 (1991).
17 Ortega, J. E. & Himpsel, F. J. Quantum well states as mediators of magnetic coupling in superlattices. *Phys. Rev. Lett.* **69**, 844–847 (1992).
18 Chang, C.-H., Dou, K.-P., Chen, Y.-C., Hong, T.-M. & Kaun, C.-C. Engineering the interlayer exchange coupling in magnetic trilayers. *Sci. Rep.* **5**, 16844 (2015).
19 Guo, G. Y. Magnetocrystalline anisotropy oscillations predicted in Fe/Au(001) superlattices. *J. Phys. Condens. Matter* **11**, 4329 (1999).
20 Przybylski, M., Dabrowski, M., Bauer, U., Cinal, M. & Kirschner, J. Oscillatory magnetic anisotropy due to quantum well states in thin ferromagnetic films (invited). *J. Appl. Phys.* **111**, 07C102 (2012).
21 Dasa, T. R., Ruiz-Daz, P., Brovko, O. O. & Stepanyuk, V. S. Tailoring magnetic properties of metallic thin films with quantum well states and external electric fields. *Phys. Rev. B* **88**, 104409 (2013).
22 Bauer, U., Przybylski, M. & Beach, G. S. D. Voltage control of magnetic anisotropy in Fe films with quantum well states. *Phys. Rev. B* **89**, 174402 (2014).
23 Lin, W.-C., Chang, P.-C., Tsai, C.-J., Shieh, T.-C. & Lo, F.-Y. Voltage-induced reversible changes in the magnetic coercivity of Fe/ZnO heterostructures. *Appl. Phys. Lett.* **104**, 062411 (2014).
24 Krupin, O., Bihlmayer, G., Starke, K., Gorovikov, S., Prieto, J. E., Döbrich, K., Blügel, S. & Kaindl, G. Rashba effect at magnetic metal surfaces. *Phys. Rev. B* **71**, 201403(R) (2005).
25 Kimura, A., Krasovskii, E. E., Nishimura, R., Miyamoto, K., Kadono, T., Kanomaru, K., Chulkov, E. V., Bihlmayer, G., Shimada, K., Namatame, H. & Taniguchi, M. Strong Rashba- type spin polarization of the photocurrent from bulk continuum states: experiment and theory for Bi (111). *Phys. Rev. Lett.* **105**, 076804 (2010).
26 Moras, P., Bihlmayer, G., Sheverdyaeva, P. M., Mahatha, S. K., Papagno, M., Sánchez-Barriga, J., Rader, O., Novinec, L., Gardonio, S. & Carbone, C. Magnetization-dependent Rashba splitting of quantum well states at the Co/W interface. *Phys. Rev. B* **91**, 195410 (2015).
27 Młyńczak, E., Eschbach, M., Borek, S., Minár, J., Braun, J., Aguilera, I., Bihlmayer, G., Döring, S., Gehlmann, M., Gospodarič, P., Suga, S., Plucinski, L., Blügel, S., Ebert, H. & Schneider, C. M. Fermi surface manipulation by external magnetic field demonstrated for a prototypical ferromagnet. *Phys. Rev. X* **6**, 041048 (2016).
28 Blum, V., Rath, Ch., Müller, S., Hammer, L., Heinz, K., Garca, J. M., Ortega, J. E., Prieto, J. E., Hernán, O. S., Gallego, J. M., Vázquez, de Parga, A, L & Miranda, R. Fe thin-film growth on Au(100): a self-surfactant effect and its limitations. *Phys. Rev. B* **59**, 15966–15974 (1999).
29 Velev, J., Sabirianov, R. F., Jaswal, S. S. & Tsymbal, E. Y. Ballistic anisotropic magnetoresistance. *Phys. Rev. Lett.* **94**, 127203 (2005).
30 Bruno, P. Tight-binding approach to the orbital magnetic moment and magnetocrystalline anisotropy of transition-metal monolayers. *Phys. Rev. B* **39**, 865–868 (1989).
31 Mokrousov, Y., Bihlmayer, G., Heinze, S. & Blügel, S. Giant magnetocrystalline anisotropies of 4d transition-metal monowires. *Phys. Rev. Lett.* **96**, 147201 (2006).
32 Cinal, M. & Edwards, D. M. Quantum-well states and magnetocrystalline anisotropy in Co/Pd structures. *Phys. Rev. B* **57**, 100–103 (1998).
33 Bauer, U., Dabrowski, M., Przybylski, M. & Kirschner, J. Experimental confirmation of quantum oscillations of magnetic anisotropy in Co/Cu(001). *Phys. Rev. B* **84**, 144433 (2011).
34 Rashba, E. I. Properties of semiconductors with an extremum loop. 1. Cyclotron and combinational resonance in a magnetic field perpendicular to the plane of the loop. *Sov. Phys. Solid State* **2**, 1109–1122 (1960).
35 Barnes, S. E., Ieda, J. & Maekawa, S. Rashba spin-orbit anisotropy and the electric field control of magnetism. *Sci. Rep.* **4**, 4105 (2014).
36 Guo, G. Y., Temmerman, W. M. & Ebert, H. First-principles determination of the magnetization direction of Fe monolayer in noble metals. *J. Phys. Condens. Matter* **3**, 8205 (1991).
37 Szunyogh, L., Újfalussy, B. & Weinberger, P. Magnetic anisotropy of iron multilayers on Au(001): first-principles calculations in terms of the fully relativistic spin-polarized screened KKR method. *Phys. Rev. B* **51**, 9552–9559 (1995).
38 Qiu, Z. Q., Pearson, J. & Bader, S. D. Asymmetry of the spin reorientation transition in ultrathin Fe films and wedges grown on Ag(100). *Phys. Rev. Lett.* **70**, 1006–1009 (1993).
39 Kawakami, R. K., Escorcia-Aparicio, E. J. & Qiu, Z. Q. Symmetry-induced magnetic anisotropy in Fe films grown on stepped Ag(001). *Phys. Rev. Lett.* **77**, 2570–2573 (1996).
40 Hahlin, A., Andersson, C., Hunter Dunn, J., Sanyal, B., Karis, O. & Arvanitis, D. Structure and magnetism of ultrathin epitaxial Fe on Ag(100). *Phys. Rev. B* **73**, 134423 (2006).
41 Khim, T.-Y., Shin, M., Park, B.-G., Lee, H. & Park, J.-H. Observation of second spin reorientation transition within ultrathin region in Fe films on Ag(001) surface. *J. Appl. Phys.* **115**, 233904 (2014).
42 Li, J., Przybylski, M., He, Y. & Wu, Y. Z. Experimental observation of quantum oscillations of perpendicular anisotropy in Fe films on Ag(1,1,10). *Phys. Rev. B* **82**, 214406 (2010).
43 Bauer, U. & Przybylski, M. Large amplitude oscillation of magnetic anisotropy engineered by substrate step density. *Phys. Rev. B* **81**, 134428 (2010).
44 Wooten, C. L., Chen, J., Mulhollan, G. A., Erskine, J. L & Markert, J. T. Direct observation of enhanced magnetic moments in Fe/Ag(100). *Phys. Rev. B* **49**, 10023–10026 (1994).
45 van der Laan, G. Microscopic origin of magnetocrystalline anisotropy in transition metal thin films. *J. Phys. Condens. Matter* **10**, 3239 (1998).
46 Manchon, A., Koo, H. C., Nitta, J., Frolov, S. M. & Duine, R. A. New perspectives for Rashba spin-orbit coupling. *Nat. Mater.* **14**, 871–882 (2015).
47 Ast, C. R., Henk, J., Ernst, A., Moreschini, L., Falub, M. C., Pacilé, D., Bruno, P., Kern, K. & Grioni, M. Giant spin splitting through surface alloying. *Phys. Rev. Lett.* **98**, 186807 (2007).
48 Dil, J. H., Meier, F., Lobo-Checa, J., Patthey, L., Bihlmayer, G. & Osterwalder, J. Rashba-type spin-orbit splitting of quantum well states in ultrathin pb films. *Phys. Rev. Lett.* **101**, 266802 (2008).

Supplementary Information accompanies the paper on the NPG Asia Materials website (http://www.nature.com/am)